ACS APPLIED MATERIALS & INTERFACES

Research Article

Cite This: ACS Appl. Mater. Interfaces 2019, 11, 23616−23622

www.acsami.org

Transparent Impact-Resistant Composite Films with Bioinspired Hierarchical Structure

Ran Chen,[†,§] Junfeng Liu,[†] Chenjing Yang,[†] David A. Weitz,[§] Haonan He,[∥] Dewen Li,[‡] Dong Chen,[*,†] Kai Liu,[*,∥] and Hao Bai[*,‡]

[†]College of Energy Engineering and [‡]College of Chemical and Biological Engineering, Zhejiang University, Zheda Road 38, Hangzhou 310027, China

[§]John A. Paulson School of Engineering and Applied Sciences, Harvard University, 11 Oxford Street, Cambridge, Massachusetts 02138, United States

[∥]Changchun Institute of Applied Chemistry, Chinese Academy of Sciences, Renmin Road 5625, Changchun 130022, China

Supporting Information

ABSTRACT: Inspired by the helicoidally organized microstructure of stomatopods' smasher dactyl club, a type of impact-resistant composite film reinforced with periodic helicoidal nanofibers is designed and fabricated, which reproduces the structural complexity of the natural material. To periodically align nanofibers in a helicoidal structure, an electrospinning system is developed to better control the alignment of electrospun nanofibers. When the nanofiber scaffold is embedded in an epoxy matrix, the presence of a hierarchical structure allows the composite films to achieve properties well beyond their constituents. The composite film exhibits excellent optical transparency and mechanical properties, such as enhanced tensile strength, ductility, and defect tolerance. With elegant design mimicking nature's hierarchical structure at multilength scales, the composite films could effectively release the impact energy and greatly increase the impact resistance, suggesting that the transparent composite films are promising protective layers suitable for various applications.

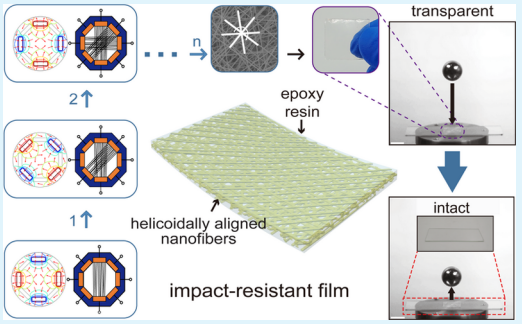

KEYWORDS: *composite film, impact resistance, bioinspired, hierarchical structure, electrospinning, nanofibers*

1. INTRODUCTION

Bioinspired innovations of composite materials have dramatically enriched the material landscape, ranging from lightweight and stiff materials mimicking bamboo to strong and tough materials resembling nacre.[1−3] Nature has been iteratively solving an optimization problem through evolution and driving the adaptation of organ functions for organism survival.[4,5] A paradigm in nature's design is to architect composite materials with hierarchical structure at different length scales, which has demonstrated excellent material properties compared to their constituents. For example, stomatopods are well known for their raptorial predatory strike, which exemplifies one of the fastest movements in nature, and their hammerlike smasher dactyl clubs, which is highly powerful to crush hard-shelled prey.[6−8] The ability of stomatopods' clubs to resist damage during a considerable impact is attributed to their composite structure consisting of a highly aligned chitinous nanofiber matrix embedded in an amorphous mineral phase. The organic chitinous nanofibers exhibit a characteristic helicoidal organization, which has been proven to be capable of dissipating impact energy by propagating microcracks.[9,10] Composite materials with such periodic helicoidal structure are thus expected to possess similar damage-tolerant property,[10−16] which have large potential in various applications.[17−21] However, such bioinspired composite materials are currently unavailable due to their structural complexity, and great challenges lie in the fabrication of nanofiber scaffolds with a periodic helicoidal arrangement.

Electrospinning has demonstrated great advantages in fabricating nanofibers. Compared with other techniques, such as drawing,[22,23] photolithography,[24] and self-assembly,[25] electrospinning could continuously fabricate mechanically strong nanofibers with controllable diameter, uniformity and morphology.[26−29] Electrospun nanofibers with more complex morphologies, such as those decorated with separated beads along the fiber,[30,31] could also be achieved when combined with microfluidic technique.[32] While electrospun nanofibers are generally nonwoven due to bending instability, previous works have demonstrated that they could be unidirectionally aligned by the design of electrodes or magnets on the collector.[33,34] However, current electrospinning system still lacks the control over the three-dimensional (3D) organization of electrospun nanofibers, which limit the design of materials with more complex hierarchical structure and thus compromise the

Received: April 13, 2019
Accepted: June 7, 2019
Published: June 7, 2019

DOI: 10.1021/acsami.9b06500
ACS Appl. Mater. Interfaces 2019, 11, 23616−23622

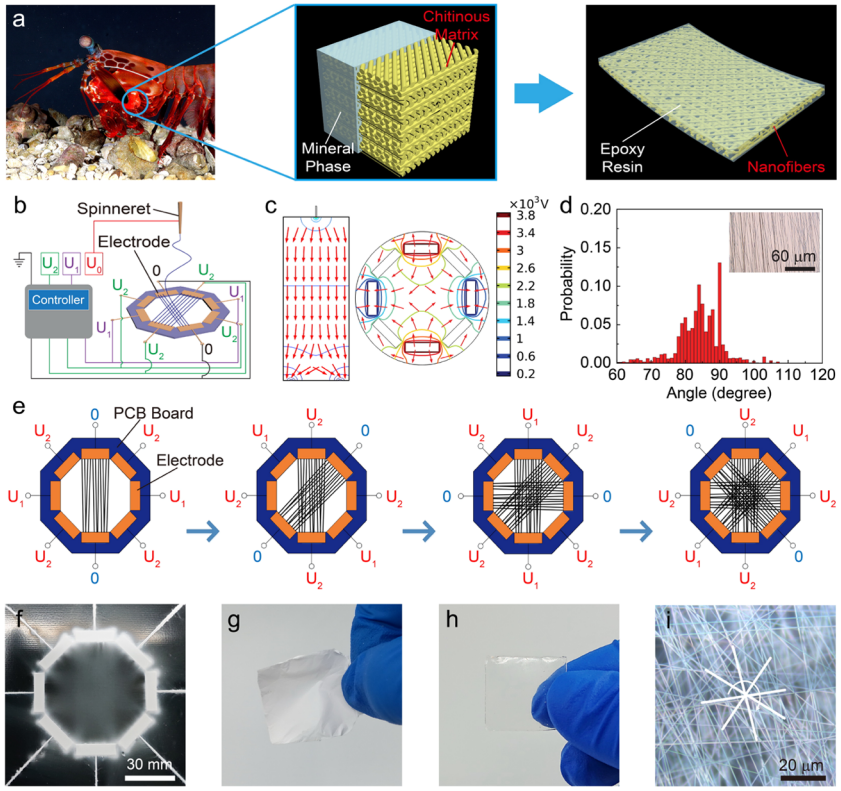

Figure 1. Bioinspired design of impact-resistant composite films. (a) A snapshot of a stomatopod with hammerlike smasher dactyl clubs. The hierarchical structure at multilength scales contributes to its excellent impact-resistant property and inspires the design of impact-resistant composite films reinforced with helicoidally aligned nanofibers. (b) Schematic illustration of the electrospinning setup with a patterned collector and a programmable voltage controller. (c) Simulation of the electric field, which is unidirectionally aligned along the two grounded electrodes. (d) Statistics of the orientations of unidirectionally aligned nanofibers, showing an order parameter of $S = \langle 2\cos^2\theta - 1\rangle \sim 0.97$. (e) Fabrication of a periodic helicoidal microstructure by alternatively aligning nanofibers along the four pairs of electrodes. (f, g) Optical images of helicoidally aligned nanofibers. (h) Transparent composite film reinforced with helicoidal nanofibers. (i) Scaffold of birefringent nanofibers imaged under depolarized optical microscope.

performance of composite materials. Advancement of electrospinning technology that enables well-defined 3D architectures is, therefore, desired.

In this paper, we develop an electrospinning system with a delicate control of applied voltages on the designed electrodes, which enables the alignment of electrospun nanofibers at multiple length scales and thus the fabrication of helicoidally aligned nanofibers that mimic the microstructure of stomatopod's hammerlike club. Composite films of hierarchical helicoidal nanofibers embedded in an epoxy matrix demonstrate excellent transparency and increased tensile strength and toughness. Due to the helicoidally aligned nanofibers, the composite films are resistive to cut propagation and show a consistent tensile strength in the presence of defects. Falling ball and pendulum impact tests prove that the composite films could effectively absorb a large amount of impact energy and greatly increase the impact resistance, suggesting promising applications of the transparent films as a protective layer in various fields, such as bendable displays and airplane windows.

2. RESULTS AND DISCUSSION

2.1. Design of Composite Films with Hierarchical Structure. Inspired by the natural microstructure of stomatopods' club, we design a hierarchical composite film reinforced with periodic helicoidal nanofibers to achieve advanced functions, such as impact resistance, as shown in Figure 1a. Helicoidally aligned nanofibers are prepared by an electrospinning system with a well-designed collector and a programmable voltage control system, as shown in Figure 1b. Four pairs of electrodes are designed on the collector with a void gap at the center. During the electrospinning process, a high potential (18 or 14 kV) is applied on the spinneret and one pair of electrodes is grounded while other three pairs are connected to high potentials (U_1 = 4 kV and U_2 = 2.5 kV, respectively). The generated electric field is mainly focused and unidirectionally aligned in the plane spanned by the high-voltage spinneret and the two grounded electrodes, as shown in Figure 1c. The electric field subsequently guides the stretching and alignment of nanofibers through electrostatic interaction along the two grounded electrodes.[35] The unidirectionally aligned nanofibers are highly ordered with an order parameter of $S = \langle 2\cos^2\theta - 1\rangle \sim 0.97$ (where θ is the angle between the individual fiber orientation and the average fiber orientation), as shown in Figure 1d and calculated in detail in the Supporting Information. After depositing the first layer of unidirectionally aligned nanofibers, the applied voltages are alternated between the electrodes, i.e., the orientation of grounded electrodes rotates clockwise, and a second layer of unidirectionally aligned nanofibers are deposited on top of the previous one with an angle of 45°. Therefore, periodic stacking of unidirectional nanofibers along each pair of electrodes constitutes a scaffold of nanofibers helicoidally aligned along four rotating directions, as shown in Figure 1e,f.

DOI: 10.1021/acsami.9b06500
ACS Appl. Mater. Interfaces 2019, 11, 23616−23622

A typical film of nanofibers consists of roughly 100 periods of helicoidal nanofibers along 4 rotating directions, as shown in Figure 1g. Composite films are then prepared by solution impregnation of epoxy resin into the nanofiber scaffold, as shown in Figure 1h. Mainly due to the small size of nanofibers (d ~ 100 nm) and the small refractive index mismatch between the nanofibers and the resin, the obtained composite film exhibits excellent optical transparency and is essentially the same as neat epoxy film, as shown in Figure S1. The scaffold of birefringent nanofibers embedded in the film could be visualized under depolarized optical microscope, as shown in Figure 1i.

To systematically study the effect of the microstructure of reinforced nanofibers and investigate their mechanical performance, we prepare composite films with three different types of nanofiber arrangements, i.e., nanofibers unidirectionally aligned along one direction (U-1) (Figure 2a), periodically aligned along two orthogonal directions (O-2) (Figure 2b), and helicoidally aligned along four rotating directions (H-4) (Figure 2c). Well-controlled alignments of nanofibers are achieved by electrospinning under a programmable voltage controller and their microstructures are clearly visualized by the scanning electron microscopy (SEM) images in Figure 2 and magnified in Figure S2. When the scaffolds of nanofibers are infiltrated with epoxy resin, the three types of composite films are all transparent and look similar. However, their mechanical performances are very different and strongly affected by the microstructure of underlying nanofibers.

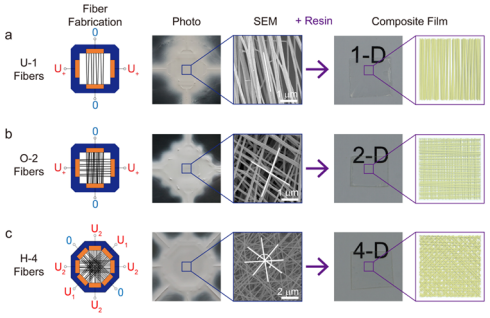

Figure 2. Fabrication of transparent composite films reinforced with different nanofiber arrays. Hierarchical structures of nanofibers (a) unidirectionally aligned along one direction (U-1), (b) periodically aligned along two orthogonal directions (O-2), and (c) helicoidally aligned along four rotating directions (H-4) are prepared by electrospinning with a patterned electrode and a programmable voltage controller. Transparent composite films are obtained by infiltrating epoxy resin into the interstitial spaces of nanofibers.

2.2. Mechanical Properties of Composite Films. To test the mechanical performance of our composite films, nylon is chosen as a model material, which has a larger tensile strength (~300 MPa) than epoxy,[36] and the results of composite films reinforced with nylon nanofibers are shown in Figure 3a. Under a typical stretching, epoxy films without nanofibers show a weak tensile strength. Since aligned nanofibers are known to be stiff and strong along the fiber direction, composite films reinforced with unidirectionally aligned nanofibers demonstrate strongly anisotropic mechanical properties, i.e., the tensile strength along the fiber direction is much larger than that perpendicular to the nanofibers. In contrast, composite films with a periodic helicoidal structure show roughly isotropic mechanical properties and overall better mechanical performances, i.e., the tensile strength and ductility of the composite films reinforced with 3 vol % nanofibers increase by 50 and 150%, respectively. These results suggest that nanofibers organized in periodic helicoidal structure could effectively improve the overall mechanical properties of the composite films.

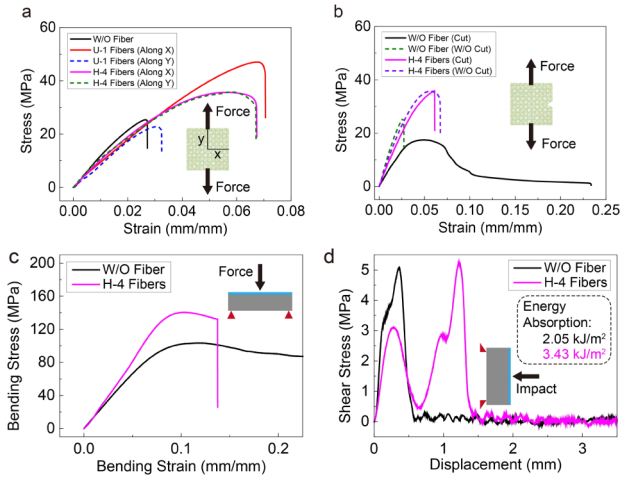

Figure 3. Mechanical performances of the composite films reinforced with nanofibers. (a) Stress−strain curves of the composite films reinforced with nylon nanofibers. The mechanical performances of the composite films strongly depend on the underlying hierarchical structure of the nanofibers. (b) Stretching tests of the composite films with a small cut. The performance of neat epoxy film is greatly compromised, while the composite films are resistive to the cut propagation, showing a consistent result. (c) Performances of the bending test on an epoxy block adhered with a composite film, showing a better bending resistance than the epoxy block alone. (d) Results of the pendulum impact test. The protective layer of the composite film absorbs a large amount of impact energy before the epoxy block.

Finite-element simulations of the composite films show consistent results with the experiments (Figure S3). The composite films with unidirectionally aligned nanofibers show a maximum tensile strength of ~50 MPa along the fiber direction and a minimum tensile strength of ~20 MPa perpendicular to the fiber direction. However, the periodic helicoidal stacking of anisotropic nanofiber layers along four rotating directions nearly contributes to an isotropic mechanical enhancement, improving the overall tensile strength up to ~39 MPa.

Defects generally exist in the microstructure of composite materials, which can weaken the performance of a material by orders of magnitude. To demonstrate the defect-tolerant property of our composite films with a periodic helicoidal microstructure, a small cut is introduced into the samples, as shown in Figure 3b. During the stretching of a sample film, the stress is easily focused on the tip of the cut, tearing the film and resulting in a great decrease of the tensile strength. Therefore, the tensile strength of epoxy films without nanofibers reduces from ~25 MPa in the absence of cut to ~17 MPa in the presence of cut, indicating that neat epoxy films are susceptible to defects and their mechanical performance could easily be compromised. In contrast, the periodic helicoidal nanofibers embedded in the resin matrix could effectively dissipate the stress on the tip of the cut.[9] Our composite films are thus resistive to the cut propagation and show a consistent tensile strength of ~36 MPa.

The preparation of the composite films is quite versatile as various kinds of nanofibers can be made by electrospinning. The overall mechanical properties of the composite films could thus be tailored by using different nanofibers as the scaffold. When

DOI: 10.1021/acsami.9b06500
ACS Appl. Mater. Interfaces 2019, 11, 23616−23622

polyurethane nanofibers are reinforced in the resin matrix, the composite films overall show a smaller tensile strength than those reinforced with nylon nanofibers, since polyurethane has a smaller tensile strength than nylon, as shown in Figure S4. Irrespective of the difference between polyurethane and nylon, both types of composite films show a similar mechanical trend when their underlying nanofiber microstructures are the same, i.e., composite films reinforced with nanofibers aligned along one direction demonstrate strongly anisotropic mechanical properties, while composite films with a periodic helicoidal structure show similar mechanical performance along different directions.

To demonstrate the capability of our composite films to resist static and dynamic forces, bending and pendulum impact tests are performed on the samples, respectively. A composite film of t = 0.5 mm thick is adhered to an epoxy block of t = 10 mm thick. The addition of the thin composite film with periodic helicoidal nanofibers exhibits a significant increase of the yield limit from 102 to 140 MPa, as shown in Figure 3c. The crack of the testing sample with a composite film may be attributed to the applied bending stress beyond its limit. The shear stress as a function of displacement during a pendulum impact is shown in Figure 3d. In the sample with a composite film, two peaks are observed, one corresponding to the protective layer and the other to the epoxy block. The area of the first peak suggests that the thin composite film absorbs a large amount of energy of 1.4 kJ/m^2 during the impact, and the gentle incline of the peak indicates that the composite film releases the impact in a continuous manner.

2.3. Impact-Resistant Performance of Composite Film.

Previous study on stomatopods' club suggests that its hybrid structure with periodic helicoidal chitinous nanofibers displays effective defense against repetitive high-energy loading events.[9] Therefore, a strengthened impact resistance is expected in our composite films. A simple falling ball test is performed to demonstrate the tolerance of the composite films to high-velocity impacts, as shown in Figure 4a, and the heights required to crack the testing films are statistically plotted in Figure 4b.

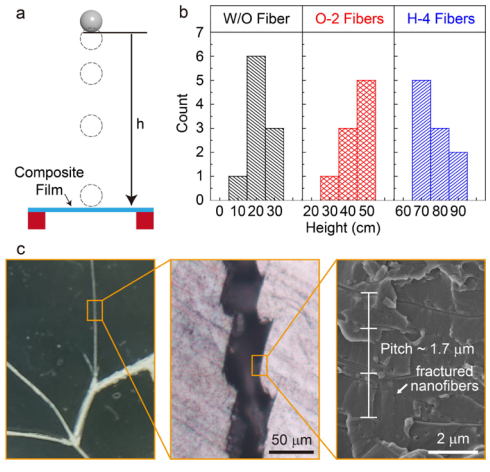

Figure 4. Impact-resistant tests of freely suspended composite films. (a) Schematic illustration of a ball freely falling from a certain height onto the composite film. (b) Statistics of the heights, at which the falling ball cracks the composite film. (c) Microscopy and SEM images of the fractures on the cracked composite films, exhibiting a typical zigzag pattern. The cross section of the fracture shows the embedded helicoidal nanofiber array with a period of $p \sim 1.7$ μm and a good interfacial adherence formed between the nanofibers and the resin.

Epoxy films without nanofibers of t = 1 mm thick generally crack when a ball of m = 0.25 kg freely falls from a height of $h \sim 20$ cm and show a smooth fracture line (Figure S5). In contrast, the required height for composite films reinforced with orthogonally aligned nanofibers increases to $h \sim 40$ cm, while composite films with helicoidally aligned nanofibers show a much better performance and require a height of $h \sim 80$ cm, proving that the helicoidal scaffold plays an important role in strengthening the impact resistance. To unveil the underlying mechanism, the fracture lines of cracked films are investigated under optical microscope, as shown in Figure 4c. Zigzag fractures are observed in the composite films with periodic helicoidal nanofibers, which is a typical evidence that the composite film resists the propagation of fractures.[2] Generally, cracks tend to follow the direction of nanofibers. However, because of the helicoidal nanofiber array, there is no preferable direction for cracks to follow; thus, cracks can only propagate through the material by finding a tortuous zigzag path, which would require greater energy to achieve complete fracture. Therefore, the biologically inspired helicoidal scaffold is shown to be an effective structure to resist fractures and stand high-energy impacts.

The composite films with enhanced mechanical properties are ideal for various applications. To test our composite films as a protective layer, a thin composite film with a thickness of t = 500 μm is adhered on top of a glass slide. When a steel ball of m = 16 g falls from a height of h = 80 cm onto the glass slide, the glass slide easily cracks without any protection (Figure 5a) or under the protection of a toughened glass film (Figure 5b) or a resin

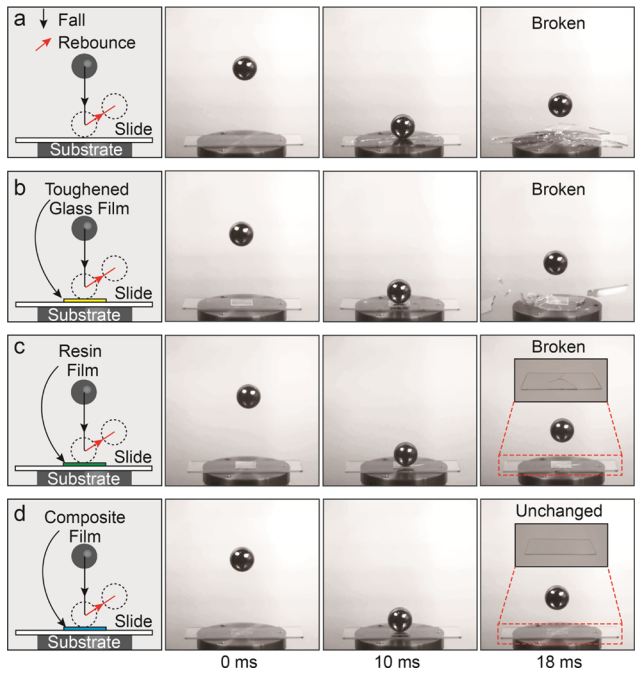

Figure 5. Performances of different films as a protective layer. (a) Without any protection, the glass slide cracks easily under the impact of a falling steel ball. (b) A layer of toughened glass film is used to protect the glass slide and both of them are cracked by the falling ball. (c) A layer of resin film could not prevent the cracking of the glass slide from the falling ball. (d) The composite film reinforced with periodic helicoidal nanofibers shows excellent impact-resistant performance, which protect the glass slide underneath from the impact of the falling ball. In all these experiments, different protection films have a same thickness of t = 500 μm and the steel ball of m = 16 g falls from a same height of h = 80 cm.

DOI: 10.1021/acsami.9b06500
ACS Appl. Mater. Interfaces 2019, 11, 23616−23622

film (Figure 5c). In contrast, the composite film reinforced with periodic helicoidal nanofibers shows excellent impact-resistant performance, which protects the glass slide underneath from cracking, as demonstrated in Figure 5d. The ability of the composite film to resist fracture is attributed to its elegant design mimicking nature's hierarchical structure at multilength scales, which displays effective defense against catastrophic failure during high-energy loading events.[9] The excellent impact-resistant performance thus suggests promising applications of the transparent composite films as a protective layer in various fields, such as bendable displays and airplane windows.

The excellent performances of the composite films are attributed to the well-controlled helicoidal arrangement of the nanofibers by electrospinning. Compared with helicoidal structures produced by other techniques, such as 3D printing or self-assembly,[15] electrospinning is advantageous for fabricating nanofibers of small size, which is important to achieve excellent optical transparency. In addition, due to the stretching and induced order, electrospun nanofibers are known to be stiffer and stronger than those prepared by extrusion, which is important to improve the overall mechanical performance of the composite film. Compared with nested structures, such as helicoidally aligned nanofibers, the composite films reinforced with helicoidally aligned nanofibers demonstrate distinguished better performances, suggesting that helicoidal structure is essential in improving the performances of the composite films and helicoidally aligned nanofibers possess the characteristics of helicoidal scaffolds in nature.

3. CONCLUSIONS

The bioinspired design of impact-resistant composite films are realized by engineering the microstructure of reinforced nanofibers. Alignments of nanofibers in a periodic helicoidal scaffold are achieved through a delicate design of the electrodes and the control of the applied voltages. The composite films with hierarchical nanofibers exhibit excellent optical transparency and enhanced mechanical properties, such as tensile strength, ductility, and toughness. The periodic helicoidal array of nanofibers are advantageous to resist the propagation of cracks and absorb a large amount of impact energy; the composite films thus show excellent performances of defect-tolerance and impact-resistance. The studies of the composite films with hierarchical nanofiber structure provide important design insights into the advancement of impact-resistant materials. The developed electrospinning technology also presents a powerful platform that enables the design and fabrication of functional materials with more complex structure at multiple length scales and thus with better performances.

4. EXPERIMENTAL SECTION

4.1. Materials. Nylon 6 (Production Number: 181110), purchased from Sigma-Aldrich, and polyurethane (Texin RxT85A), bought from Covestro, are used to fabricate nanofibers by electrospinning. Formic acid, dimethylformamide, and tetrahydrofuran are purchased from Sinopharm Reagent and used as solvents. Bisphenol-F epoxy resin (Hexion EPON Resin 862) is used to prepare composite films and epoxy blocks. Poly(propylene glycol) bis(2-aminopropyl ether) ($M_n \sim$ 230 Da, purchased from Aladdin) is used to cross-link the epoxy resin. The epoxy resin and the cross-linker are mixed at a weight ratio of 2:1 and cured in an oven at 60 °C for 48 h.

4.2. Fabrication of Ordered Nanofibers. A syringe pump (LongerPump LSP01-1A) is used to continuously infuse the polymer solution into the conductive spinneret and a PCB board with four pairs of electrodes is used as the collector. The distance between each pair of electrode is 60 mm. In a typical experiment, the infusion rate of the polymer solution is 0.4 mL/h and the distance between the spinneret and the collector is 15 cm. The electrospinning experiments are carried out at room temperature (~20 °C), and the humidity is maintained below 50%. Three power supplies (HB-Z303-1AC brought from Tianjin HENGBO Technology Development Co.) are used to fabricate nanofibers helicoidally aligned along four rotating directions. All the three power supplies are commonly grounded. One power supply (U_0) is directly connected to the spinneret. Each of the rest two power supplies (U_1 and U_2) is connected to the four pairs of electrodes on the collector via four relays. The ground is also connected to the four pairs of electrodes via four relays. Therefore, there are total 12 relays. The voltage applied on each pair of electrodes is controlled by the on or off of each relay, while each relay is controlled by each channel of the programmable controller. At each moment, by programing the programmable controller, the output of the programmable controller through each channel could control the on or off of each relay to achieve one pair of electrodes connected to U_1, two pairs connected to U_2, and the last pair grounded, as shown in Figure 1b. By programing the programmable controller over time, it is achievable to periodically alternate the voltages applied on the electrodes and rotate the grounded electrodes clockwise at an interval of desired minutes. Therefore, the connection between the electrodes on the collector and the power supplies is controlled by the programmable controller.

For nylon nanofibers, 20 wt % nylon solution is prepared by dissolving nylon in formic acid and 18 kV is applied on the spinneret. To fabricate helicoidally aligned nanofibers, one pair of electrodes is grounded. The voltage applied on the two pairs of electrodes close to the grounded one is 2.5 kV, and the voltage applied on the last pair perpendicular to the grounded one is 4 kV. The voltages applied on the electrodes are periodically alternated, and the grounded pair of electrodes rotates clockwise at an interval of 2 min. A typical film of helicoidally aligned nanofibers is prepared by continuous electrospinning for 1 day. To fabricate orthogonally aligned nanofibers, two pairs of electrodes are designed on the collector. One pair is grounded and the other is connected to 4 kV. The applied voltages on the electrodes switch between the two pairs of electrodes every 2 min. A typical film of orthogonally aligned nanofibers is prepared by continuous electrospinning for 1 day. To fabricate polyurethane nanofibers, 20 wt % polyurethane solution is prepared by dissolving polyurethane in the mixture of dimethylformamide and tetrahydrofuran (ratio of dimethylformamide/tetrahydrofuran = 1:1), and 14 kV is applied on the spinneret. All other parameters are the same as those used for nylon nanofibers.

4.3. Characterization and Test of Composite Films. Optical micrographs are taken by an optical microscope (Sunny CX40P). SEM images are captured using Hitachi S4800. The stretching and bending tests are carried out by a universal testing machine (Instron 5944). The samples are 20 mm × 20 mm wide and 1 mm thick. The volume of the nanofiber scaffold is measured by Archimedes' drainage method and the volume fraction of the nanofiber scaffold in the composite film is kept at a constant of 3 vol %. The cross-head speeds are 1 mm/min in the stretching experiment and 0.5 mm/min in the bending experiment. The artificial small cut is an equilateral triangle with a depth of 2 mm into the edge of the sample. The impact ductility test is carried out using a falling ball impact testing machine (JINCHE LX-2000A). The weight of the ball is 0.25 kg. The height of the falling ball starts from 0.1 m and increases gradually with an interval of 0.1 m, until the falling ball cracks the composite film. In the pendulum impact test, the testing samples are simply supported in the machine (CEAST 9050) and tested using a 7.5 J pendulum.

4.4. Finite-Element Simulation of Composite Films. Numerical analysis of the stress−strain performance of the composite films is carried out by finite-element simulation. ACP module in ANSYS software is used in the simulation. The model composite film is 10 mm × 10 mm wide and 1 mm thick. The parameters of the composite films are set according to the experimental results. The Young's module is 1024 MPa for epoxy resin matrix alone, 777.48 MPa for U-1 nanofibers along the fiber direction, 890.596 MPa for U-1 nanofibers perpendicular to the fiber direction, and 607.9 MPa for H-4 nanofibers

DOI: 10.1021/acsami.9b06500
ACS Appl. Mater. Interfaces 2019, 11, 23616−23622

along all directions. The Poisson's ratio is 0.34 for all films. The rigidity modulus is 387.88 MPa for epoxy resin matrix alone, 294.5 MPa for U-1 nanofibers along the fiber direction, 337.33 MPa for U-1 nanofibers perpendicular to the fiber direction, and 230.MPa for H-4 nanofibers along all directions. The breaking strength is 24.27 MPa for epoxy resin matrix alone, 40.5 MPa for U-1 nanofibers along the fiber direction, 20.27 MPa for U-1 nanofibers perpendicular to the fiber direction, 38.25 MPa for O-2 nanofibers along or perpendicular to the fiber direction, and 40.08 MPa for H-4 nanofibers along all directions. Model of reinforced nanofibers is constructed by stacking layers of oriented nanofibers in a periodic helicoidal structure. In each layer, nanofibers are unidirectionally aligned and their orientation rotates clockwise along the helical axis. Perfect adhesion is assumed between the nanofibers and the epoxy resin matrix in the simulation. The pitch of the nanofibers and the size of the composite films are consistent with the experiments. To simulate the stretching, the displacement is loaded on one side of the composite film when the other side is fixed. The relationships between the stress and strain during the stretching process are then obtained.

■ ASSOCIATED CONTENT

Supporting Information

The Supporting Information is available free of charge on the ACS Publications website at DOI: 10.1021/acsami.9b06500.

Calculation of the 2D order parameter of electrospun nanofibers; transparency of an epoxy film without nanofibers and a composite film with helicoidally aligned nanofibers; SEM image of electrospun nanofibers aligned along one direction, two orthogonal directions and four rotating directions; finite-element simulations of the composite films; stress−strain curves of composite films reinforced with polyurethane nanofibers; microscope images of fractures on neat epoxy films, showing a smooth fracture line (PDF)

Impact-resistant performances of different protection films (AVI)

■ AUTHOR INFORMATION

Corresponding Authors

*E-mail: chen_dong@zju.edu.cn (D.C.).
*E-mail: kai.liu@ciac.ac.cn (K.L.).
*E-mail: hbai@zju.edu.cn (H.B.).

ORCID

Ran Chen: 0000-0003-1052-3510
David A. Weitz: 0000-0001-6678-5208
Dong Chen: 0000-0002-8904-9307
Kai Liu: 0000-0003-0878-5191
Hao Bai: 0000-0002-3348-6129

Notes

The authors declare no competing financial interest.

■ ACKNOWLEDGMENTS

This work is supported by "the Fundamental Research Funds for the Central Universities" (2018QNA4046) and the National Natural Science Foundation of China (Grant Nos. 11704331 and 21878258).

■ REFERENCES

(1) Wegst, U. G. K. Bamboo and Wood in Musical Instruments. *Annu. Rev. Mater. Res.* **2008**, *38*, 323−349.
(2) Gu, G. X.; Takaffoli, M.; Buehler, M. J. Hierarchically Enhanced Impact Resistance of Bioinspired Composites. *Adv. Mater.* **2017**, *29*, No. 1700060.
(3) Yaraghi, N. A.; Kisailus, D. Biomimetic Structural Materials: Inspiration from Design and Assembly. *Annu. Rev. Phys. Chem.* **2018**, *69*, 23−57.
(4) Wegst, U. G. K.; Bai, H.; Saiz, E.; Tomsia, A. P.; Ritchie, R. O. Bioinspired Structural Materials. *Nat. Mater.* **2015**, *14*, 23−36.
(5) Gu, G. X.; Dimas, L.; Qin, Z.; Buehler, M. J. Optimization of Composite Fracture Properties: Method, Validation, and Applications. *J. Appl. Mech.* **2016**, *83*, No. 071006.
(6) Schram, F. R. Paleozoic Proto-Mantis Shrimp Revisited. *J. Paleontol.* **2007**, *81*, 895−916.
(7) Currey, J. D.; Nash, A.; Bonfield, W. Calcified Cuticle in the Stomatopod Smashing Limb. *J. Mater. Sci.* **1982**, *17*, 1939−1944.
(8) Ahyong, S. T. Phylogenetic Analysis of the Stomatopoda (Malacostraca). *J. Crustacean Biol.* **1997**, *17*, 695−715.
(9) Weaver, J. C.; Milliron, G. W.; Miserez, A.; Evans-Lutterodt, K.; Herrera, S.; Gallana, I.; Mershon, W. J.; Swanson, B.; Zavattieri, P.; DiMasi, E.; et al. The Stomatopod Dactyl Club: A Formidable Damage-Tolerant Biological Hammer. *Science* **2012**, *336*, 1275−1280.
(10) Grunenfelder, L. K.; Milliron, G.; Herrera, S.; Gallana, I.; Yaraghi, N.; Hughes, N.; Evans-Lutterodt, K.; Zavattieri, P.; Kisailus, D. Ecologically Driven Ultrastructural and Hydrodynamic Designs in Stomatopod Cuticles. *Adv. Mater.* **2018**, *30*, No. 1705295.
(11) Bouligand, Y. Sur L'existence de "pseudomorphoses Cholestériques" Chez Divers Organismes Vivants. *J. Phys. Colloq.* **1969**, *30*, C4-C90−C4-C103.
(12) Huang, Z. M.; Zhang, Y. Z.; Kotaki, M.; Ramakrishna, S. A Review on Polymer Nanofibers by Electrospinning and Their Applications in Nanocomposites. *Compos. Sci. Technol.* **2003**, *63*, 2223−2253.
(13) Livolant, F.; Giraud, M. M.; Bouligand, Y. A Goniometric Effect Observed in Sections of Twisted Fibrous Materials. *Biol. Cellulaire* **1978**, *31*, 159−168.
(14) Suksangpanya, N.; Yaraghi, N. A.; Pipes, R. B.; Kisailus, D.; Zavattieri, P. Crack Twisting and Toughening Strategies in Bouligand Architectures. *Int. J. Solids Struct.* **2018**, *150*, 83−106.
(15) Yang, Y.; Chen, Z.; Song, X.; Zhang, Z.; Zhang, J.; Shung, K. K.; Zhou, Q.; Chen, Y. Biomimetic Anisotropic Reinforcement Architectures by Electrically Assisted Nanocomposite 3D Printing. *Adv. Mater.* **2017**, *29*, No. 1605750.
(16) Zaheri, A.; Fenner, J. S.; Russell, B. P.; Restrepo, D.; Daly, M.; Wang, D.; Hayashi, C.; Meyers, M. A.; Zavattieri, P. D.; Espinosa, H. D. Revealing the Mechanics of Helicoidal Composites through Additive Manufacturing and Beetle Developmental Stage Analysis. *Adv. Funct. Mater.* **2018**, *28*, No. 1803073.
(17) Sun, W.; Cai, Q.; Li, P.; Deng, X.; Wei, Y.; Xu, M.; Yang, X. Post-Draw PAN−PMMA Nanofiber Reinforced and Toughened Bis-GMA Dental Restorative Composite. *Dent. Mater.* **2010**, *26*, 873−880.
(18) Ifuku, S.; Morooka, S.; Morimoto, M.; Saimoto, H. Acetylation of Chitin Nanofibers and Their Transparent Nanocomposite Films. *Biomacromolecules* **2010**, *11*, 1326−1330.
(19) Guo, C.; Zhou, L.; Lv, J. Effects of Expandable Graphite and Modified Ammonium Polyphosphate on the Flame-Retardant and Mechanical Properties of Wood Flour-Polypropylene Composites. *Polym. Polym. Compos.* **2013**, *21*, 449−456.
(20) Liao, H.; Wu, Y.; Wu, M.; Zhan, X.; Liu, H. Aligned Electrospun Cellulose Fibers Reinforced Epoxy Resin Composite Films with High Visible Light Transmittance. *Cellulose* **2012**, *19*, 111−119.
(21) Albers, R. G.; Nordman, P. S. Composite Single Pane Window for an Aircraft and Method of Making Same. U.S. Patent US7,968,170, 2011.
(22) Ondarçuhu, T.; Joachim, C. Drawing a Single Nanofibre over Hundreds of Microns. *EPL* **1998**, *42*, 215−220.
(23) Nain, A. S.; Amon, C.; Sitti, M. Proximal Probes Based Nanorobotic Drawing of Polymer Micro/Nanofibers. *IEEE Trans. Nanotechnol.* **2006**, *5*, 499−510.
(24) Sun, Y.; Khang, D.-Y.; Hua, F.; Hurley, K.; Nuzzo, R. G.; Rogers, J. A. Photolithographic Route to the Fabrication of Micro/Nanowires of III-V Semiconductors. *Adv. Funct. Mater.* **2005**, *15*, 30−40.

DOI: 10.1021/acsami.9b06500
ACS Appl. Mater. Interfaces 2019, 11, 23616−23622

(25) Hartgerink, J. D. Self-Assembly and Mineralization of Peptide-Amphiphile Nanofibers. *Science* **2001**, *294*, 1684−1688.
(26) Chen, R.; Liu, J.; Sun, Z.; Chen, D. Functional Nanofibers with Multiscale Structure by Electrospinning. *Nanofabrication* **2018**, *4*, 17−31.
(27) Zhang, L.; Aboagye, A.; Kelkar, A.; Lai, C.; Fong, H. A Review: Carbon Nanofibers from Electrospun Polyacrylonitrile and Their Applications. *J. Mater. Sci.* **2014**, *49*, 463−480.
(28) Li, P.; Shang, Z.; Cui, K.; Zhang, H.; Qiao, Z.; Zhu, C.; Zhao, N.; Xu, J. Coaxial Electrospinning Core-Shell Fibers for Self-Healing Scratch on Coatings. *Chin. Chem. Lett.* **2019**, *30*, 157−159.
(29) Zhao, Y.-Q.; Wang, H.-Y.; Qi, L.; Gao, G.-T.; Ma, S.-H. "Soggy Sand" Polymer Composite Nanofiber Membrane Electrolytes for Lithium Ion Batteries. *Chin. Chem. Lett.* **2013**, *24*, 975−978.
(30) Menini, R.; Farzaneh, M. Production of Superhydrophobic Polymer Fibers with Embedded Particles Using the Electrospinning Technique. *Polym. Int.* **2008**, *57*, 77−84.
(31) Díaz, J. E.; Barrero, A.; Márquez, M.; Loscertales, I. G. Controlled Encapsulation of Hydrophobic Liquids in Hydrophilic Polymer Nanofibers by Co-Electrospinning. *Adv. Funct. Mater.* **2006**, *16*, 2110−2116.
(32) Song, Y.; Chan, Y. K.; Ma, Q.; Liu, Z.; Shum, H. C. All-Aqueous Electrosprayed Emulsion for Templated Fabrication of Cytocompatible Microcapsules. *ACS Appl. Mater. Interfaces* **2015**, *7*, 13925−13933.
(33) Bazbouz, M. B.; Stylios, G. K. Alignment and Optimization of Nylon 6 Nanofibers by Electrospinning. *J. Appl. Polym. Sci.* **2008**, *107*, 3023−3032.
(34) Doshi, J.; Reneker, D. H. In Electrospinning Process and Applications of Electrospun Fibers, Conference Record of the 1993 IEEE Industry Applications Conference Twenty-Eighth IAS Annual Meeting, IEEE, 1993; Vol. *35*, pp 1698−1703.
(35) Li, D.; Wang, Y.; Xia, Y. Electrospinning of Polymeric and Ceramic Nanofibers as Uniaxially Aligned Arrays. *Nano Lett.* **2003**, *3*, 1167−1171.
(36) Bazbouz, M. B.; Stylios, G. K. The Tensile Properties of Electrospun Nylon 6 Single Nanofibers. *J. Polym. Sci., Part B: Polym. Phys.* **2010**, *48*, 1719−1731.

DOI: 10.1021/acsami.9b06500
ACS Appl. Mater. Interfaces 2019, 11, 23616−23622